Advances in the Detection and Analysis of Fog at Night Using GOES Multispectral Infrared Imagery

GARY P. ELLROD

Satellite Applications Laboratory (NOAA/NESDIS), Washington, D.C.

(Manuscript received 10 November 1994, in final form 5 April 1995)

ABSTRACT

A technique is described for the detection of fog and low clouds at night using multispectral infrared (IR) imagery from Geostationary Operational Environmental Satellites (GOES). The technique requires subtraction and enhancement of digital data from IR window channels at 3.9- and 10.7–11.2-μm wavelengths. Resulting images show stratiform clouds over any type of terrain for a wide range of surface temperature conditions. The bispectral difference images are a considerable improvement over the use of enhanced images for a single window IR channel. An image enhancement technique that displays the approximate depth of fog was developed based on the correlation of brightness differences in the two IR channels to cloud-top heights reported by aircraft. The improved resolution and greater frequency provided by the GOES I-M satellites will result in a substantial improvement in the ability to monitor areas of reduced ceilings and visibilities at night.

1. Introduction

The detection and short-range forecasting of fog and low stratus clouds at night pose a difficult problem for aviation and marine meteorologists. The number of surface-observing sites over land is insufficient to determine the true extent of fog, since many of these stations reduce operations at night. Weather reports from ocean-going vessels are usually made at six-hourly intervals and are concentrated on major shipping lanes. Because of the low density of these surface observations, especially at night, remote sensing techniques must be used to determine the coverage of fog and low clouds.

The proximity of a bank of fog to an airfield or ship is important information since it indicates the likelihood that reduced visibilities will soon occur. Once dense fog is observed at a location, it is also important to know its horizontal extent in order to estimate the time when it will dissipate from solar heating or advect downstream in the low-level flow. Using daylight visible imagery, Gurka (1978a) observed that radiation fog over land usually dissipates from the outer edges inward. Clearing will thus occur sooner if the station is located close to the edge of the fog bank (especially the upwind edge). Information on fog thickness is another parameter that can be used to estimate dissipation time. The thicker a fog layer is, the longer the time required for clearing. Thus, knowledge of the location, movement, and thickness of fog and stratus clouds during the predawn hours is critical for short-range forecasts.

Infrared (IR) imagery from geostationary weather satellites such as the Geostationary Operational Environmental Satellite (GOES) operated by the United States is the primary tool for fog detection at night due to its relatively high frequency (30 min or less). The spatial resolution of the GOES longwave IR window channel (11.2-μm) was limited to 6.9 km at the satellite subpoint, but the advanced GOES I-M series improves the resolution by nearly a factor of two (Menzel and Purdom 1994). Both sensors have sufficient resolution for fog detection at night. The greatest difficulty in the use of a single IR window channel is that the thermal contrast between fog and surrounding clear regions before sunrise is often insufficient for proper detection, even with the use of image enhancement and animation techniques.

This paper describes a technique that uses two GOES IR window channels at different wavelengths to identify regions of fog or low stratiform clouds at night regardless of existing surface temperatures. A method of estimating fog thickness from this data will also be described. An example of the effectiveness of this technique will first be shown for a case of fog over a flat coastal plain using multispectral IR data from *GOES-7*. The second example will compare the capabilities of *GOES-7* and the advanced *GOES-8* satellite in detecting fog in the Appalachian Mountains of the eastern United States.

Corresponding author address: Gary P. Ellrod, Satellite Applications Laboratory, USDOC/NOAA, NESDIS, Washington, DC 20233.
E-mail: gellrod@orbit.nesdis.noaa.gov

2. Background

a. *Radiative properties of clouds*

Differences in the radiative properties of clouds observed in various visible and IR wavelengths were determined theoretically by Hunt (1973). It was found that clouds observed in a short wavelength (3.8 μm) IR window (hereafter referred to as SIR) had a significantly lower emissivity[1] than at the longwave (11.0 μm) IR (LIR) window for clouds containing either water droplets or ice particles. The variation of emissivity versus height above cloud base (i.e., cloud thickness) in the two IR channels and their differences for a stratocumulus cloud are shown in Fig. 1. Emissivity differences are shown to be generally 20%–40% for significant cloud depths.

The temperature difference (ΔT) of a cloud observed by a satellite radiometer in the LIR and SIR wavelengths is mainly due to the emissivity differences described above. There is also a small contribution from transmissivity differences that allow more radiation from below the cloud top to be sensed in the SIR channel. Since the tops of stratus clouds are within inversion layers (Findlater 1985), this results in cooler observed IR temperatures. Both factors result in liquid stratiform clouds appearing colder at night in the SIR channel than in the LIR channel. The difference is most pronounced for clouds with small droplets such as radiation fog. Thin ice-phase cirrus clouds, on the other hand, appear warmer in the SIR window because of much higher transmissivity. In cloud-free regions, the ΔT between the two channels is usually small (<2 K) and is due to differential water vapor absorption. Although ΔTs associated with fog and stratus are small ($\approx$2–5 K), they are sufficient to provide clear discrimination of the cloud edge in most cases if the IR images are properly enhanced and displayed.

During daylight hours, there is a strong contribution to the total observed radiance in the 3.9-μm wavelength from sunlight backscattered by liquid water clouds. The reflected sunlight overwhelms the thermal differences of clouds normally observed in the window IR channels. As a result, the use of two window channels for fog detection is not effective during hours of sunlight. It is not necessary during daylight, however, since fog and stratus clouds have distinctive characteristics in high-resolution (1 km) GOES visible imagery (e.g., Anderson et al. 1974). A situation where the SIR imagery can be useful during daylight is in distinguishing low clouds from snow cover. The reflectance of sunlight off a snow-covered surface in SIR is much smaller than that for liquid water clouds (Kidder and Wu 1984; Allen et al. 1990). This difference results in improved brightness contrast between the clouds and snow cover. This contrast is often better than the thermal contrast seen in the LIR channel.

b. *Use of multispectral IR from NOAA AVHRR*

The use of the bispectral technique for the specific purpose of nighttime fog detection was first accom-

[1] Emissivity is the ratio of emitted radiance to blackbody radiance at a given temperature. A thick cloud layer has an emissivity close to 1.0 when seen in the long-wave (11–12 μm) IR window.

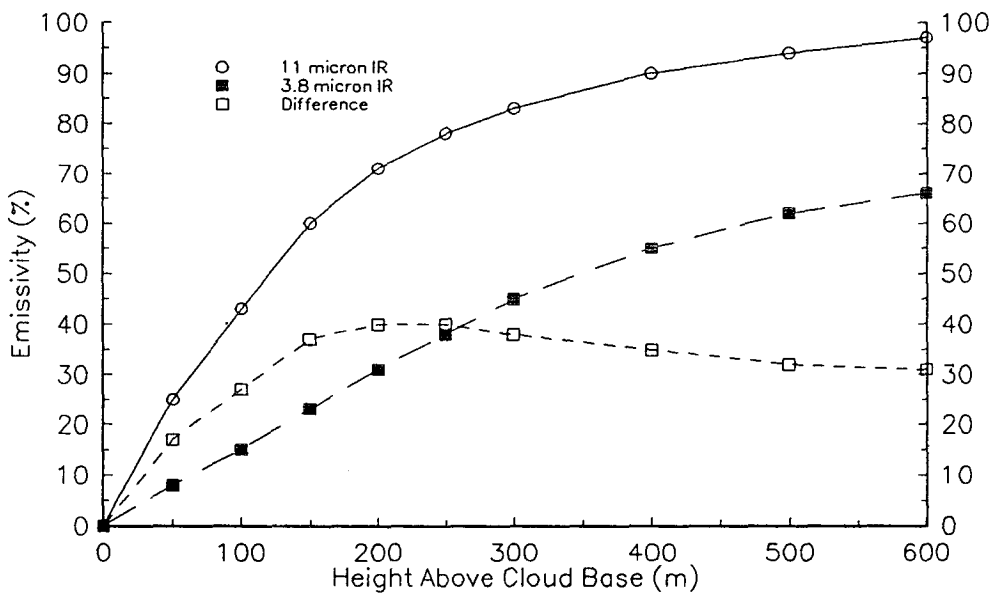

FIG. 1. The variation of emissivity (%) in a stratocumulus cloud of water content 0.1 gm^{-3} for increasing height above cloud base (m). Emissivities are shown for longwave (LW) IR channel (11 μm), the shortwave (SW) channel (3.8 μm), and the difference between the two (from Hunt 1973).

plished in Great Britain (Eyre et al. 1984). Imagery was used from the Advanced Very High Resolution Radiometer (AVHRR) onboard the NOAA (National Oceanic and Atmospheric Administration) polar-orbiting satellites. The AVHRR produces imagery in five spectral bands (three IR, one visible, one near IR) with a spatial resolution of 1.1 km. Eyre et al. (1984) used the following channels for fog detection: channel 3 centered near 3.7 μm, and channel 4 at 11.0 μm. Temperature differences greater than or equal to 2.5 K were assumed to represent opaque cloud layers. For differences less than 0.5 K, clouds were assumed to be absent, and colors were assigned to discriminate land–water boundaries and other low-level features. Intermediate temperature differences were related to pixels (picture elements) that were partially filled with cloud or contained semitransparent fog or cloud within a whole pixel. Prior to this work, AVHRR channels 3, 4, and 5 were used to flag and remove cloudy pixels and to improve the accuracy of global sea surface temperatures (e.g., McClain et al. 1983).

In the United States, a similar approach was used with AVHRR data (d'Entremont 1986; d'Entremont and Thomason 1987). Additional information was obtained from channel 5 (12.0 μm) to produce a color composite image that highlighted several different cloud types, including thin cirrus.

3. Availability and use of GOES multispectral IR

The bispectral fog-detection capability has more recently been demonstrated to be feasible using the lower resolution imagery from *GOES-7* (Ellrod et al. 1989; Ellrod 1991). The radiometer onboard *GOES-7* is called the Visible and Infrared Spin Scan Radiometer (VISSR) Atmospheric Sounder (VAS) (Montgomery and Uccellini 1985). Window IR data at 11.2 μm is available from GOES–VAS in channel 8 (hereafter CH8). CH8 is produced every 30 min with a subpoint resolution of 6.9 km (8–10 km at midlatitudes). An equivalent to the AVHRR channel 3 is GOES-VAS channel 12 (3.9 μm) (CH12). CH12 has a subpoint resolution of only 13.8 km (16–19 km at midlatitudes), but it can still be used to derive imagery for detection of large regions of fog or low clouds. However, the poor resolution of GOES-VAS usually does not permit observation of fog that occurs in narrow valleys.

The CH12 imagery from *GOES-7* is always produced during the sounding mode of operation that obtains IR data in all 12 VAS channels. The most useful CH12 data are obtained during the MultiSpectral Imaging (MSI) mode in which three channels (normally including the 11.2-μm window and 6.7-μm water vapor) are available. CH12 in the MSI mode has been available hourly since February 1992 when the StormFest Project required this data for cloud-phase studies. Even with the hourly interval, animation of the imagery can still be used to observe progressive changes in low cloud cover at night.

The first satellite in the advanced GOES I-M series, designated *GOES-8* after attaining orbit, was launched in April 1994. *GOES-8* provides 3.9- and 10.7-μm IR imagery (CHs 2 and 4, respectively) with a subpoint resolution of 4.0 km (5–6 km at midlatitudes). The improvement in resolution of *GOES-8* over *GOES-7* is more than three times better in the SIR channel and twice as good in the LIR. Since the *GOES-8* has independent imager and sounder instruments, it does not have the constraints that *GOES-7* has with respect to multispectral imaging. The 3.9-μm imagery is available at a minimum of every 15–30 min, compared to hourly at best with *GOES-7* CH12. Another improvement is that instrument noise has been reduced slightly in both channels. These factors result in much better detection and animation capabilities from *GOES-8* and beyond. For a detailed description and comparison of the *GOES-8* and *GOES-7* satellites, see Menzel and Purdom (1994).

4. Image processing

For the past several years, bispectral difference imagery derived from LIR and SIR data was routinely produced for experimental use several times nightly from *GOES-7* or *GOES-8* at the NOAA Science Center in Camp Springs, Maryland. The images are currently processed hourly from 0630 to 1030 UTC (corresponding to 0130 to 0630 Eastern Standard Time) on a Man-computer Interactive Data Analysis System (McIDAS) (Suomi et al. 1983). There are interruptions in this schedule from 0630 to 0800 UTC near the spring and fall equinoxes due to satellite eclipse.[2] By producing a series of images, animation can be used to clearly show changes in fog coverage. After the raw digital image data are received, a program digitally subtracts brightness values in the LIR channel from those in the SIR channel. In this format, warm (cold) temperatures correspond to dark (light) image brightness values. Positive values are assigned to locations where the SIR channel is colder than LIR. Although raw 10-bit

[2] Satellite eclipse occurs near the spring and autumnal equinoxes when the satellite is in the earth's shadow and cannot recharge its onboard batteries. Imaging and sounding functions are shut down at those times.

TABLE 1. Assigned output image brightness.

CH8–CH12 counts	Output brightness counts
—	—
+2	136
+1	132
0	128
−1	124
−2	120
. . . etc	. . . etc

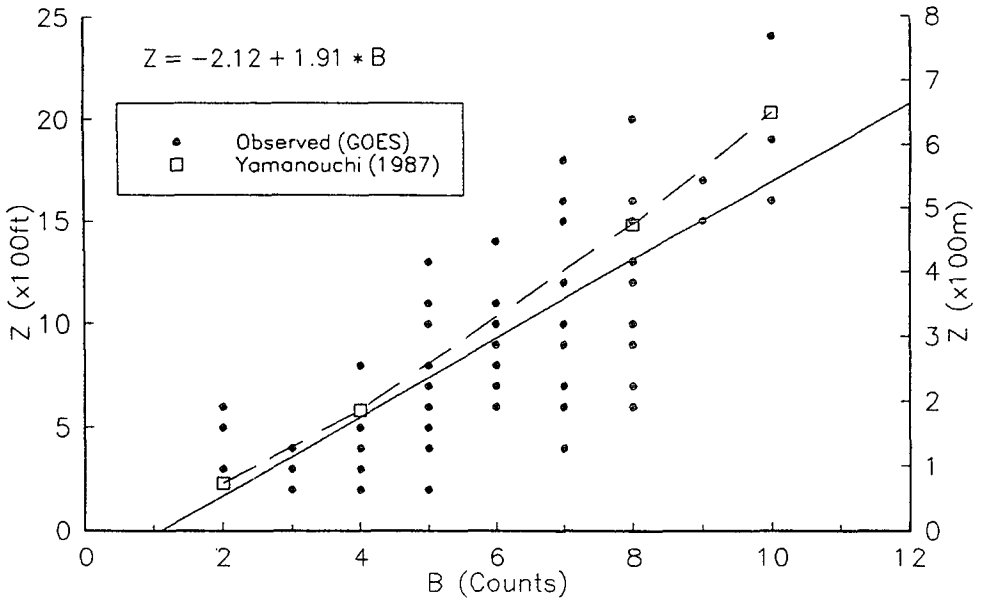

FIG. 2. Fog depth (ft and m) versus brightness differences (counts) between GOES IR CH12 (3.9 μm) and CH8 (11 μm). A least-squares regression line of best fit and its equation are shown. One count is approximately 0.5 K. Data from Yamanouchi et al. (1987) are shown for comparison.

GOES-8 IR data are calibrated differently, it is converted to an 8-bit format similar to *GOES-7*. This conversion allows for more rapid processing on McIDAS.

The brightness differences (in digital counts) are then modified for improved display according to the conversion shown in Table 1. Small changes in brightness become more easily observed because they are inflated and placed in the middle range of the 0–255-count gray scale. A difference of two digital counts in the *GOES-7* IR data corresponds to approximately 1.0 K (Clark 1983).

A smoothing program can then be used to reduce the noise inherent to the SIR channel image data from

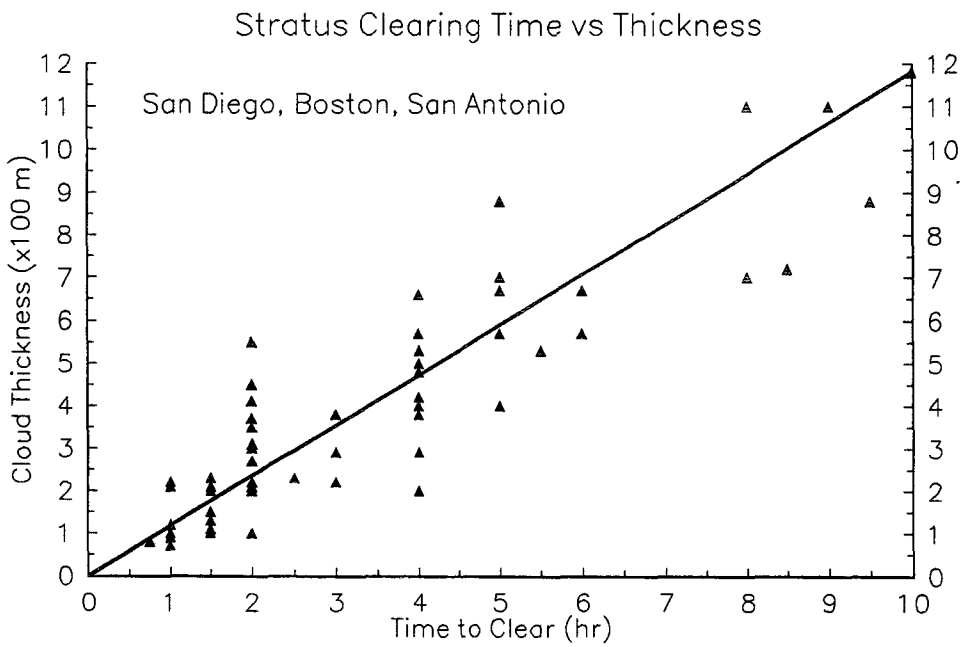

FIG. 3. Relationship between time required for clearing of stratus clouds (hours) versus the depth of the fog (×100 meters) determined from aircraft at three locations (after Wood 1938).

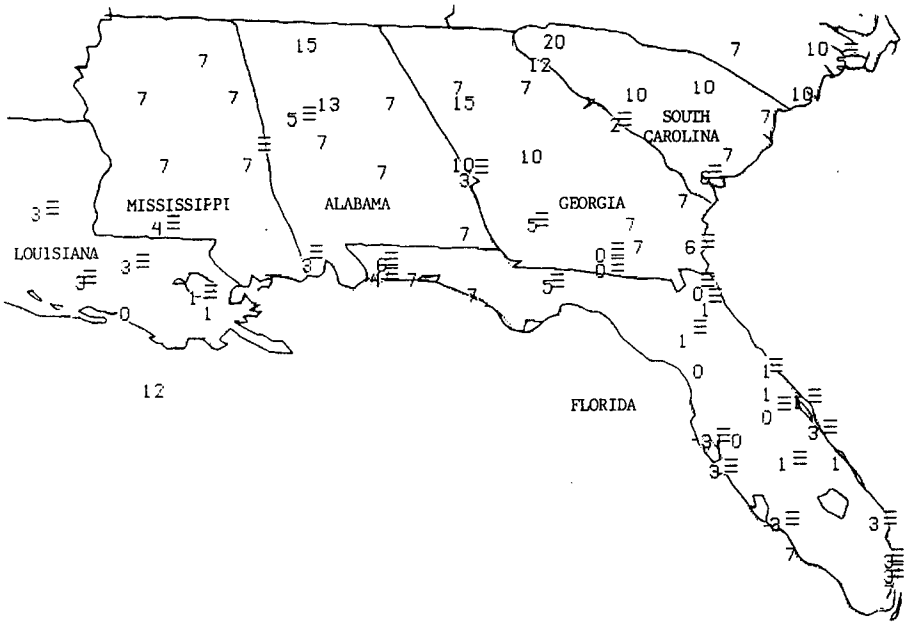

FIG. 4. Observed surface weather and visibility (miles) at 1100 UTC 26 October 1992. The symbol ≡ represents fog.

either GOES. The smoothing program determines the brightness value at any pixel by computing a center-weighted average for a 3 × 3 or 5 × 5 array. A lookup table is then applied to the final image to further improve the contrast on the video display.

A version of the bispectral difference imagery is also in use at the National Aviation Weather Advisory Unit (NAWAU), a branch of the United States National Weather Service (NWS) in Kansas City, Missouri. The imagery is used to obtain information on the extent of low clouds for aviation Area Forecasts (FAs) and short-range advisories referred to as AIRMETs. Unfortunately, the bispectral product is not yet distributed widely to users in the United States; it is primarily available at large forecast centers such as those in Washington, DC, Miami, Florida, and Kansas City, Missouri, and selected smaller offices.

The primary means of producing satellite imagery for transmission to NWS offices [the GOES Sectorizer System (GSS)] does not have the capability of producing bispectral difference imagery directly. Thus, it must be generated on another system. A new PC-based display system, called RAMSDIS (RAMM Advanced Meteorological Satellite Demonstration and Interpre-

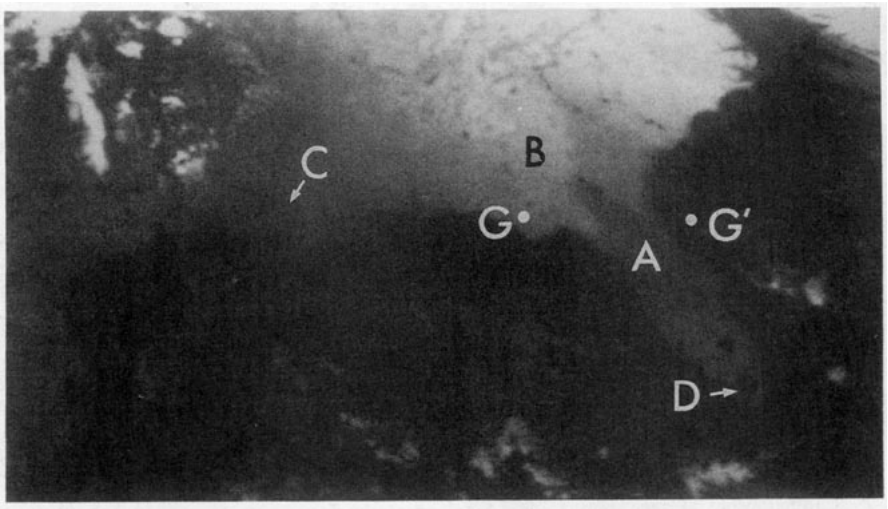

FIG. 5. *GOES-7* CH8 (11.2 μm) IR image at 1130 UTC 26 October 1992.

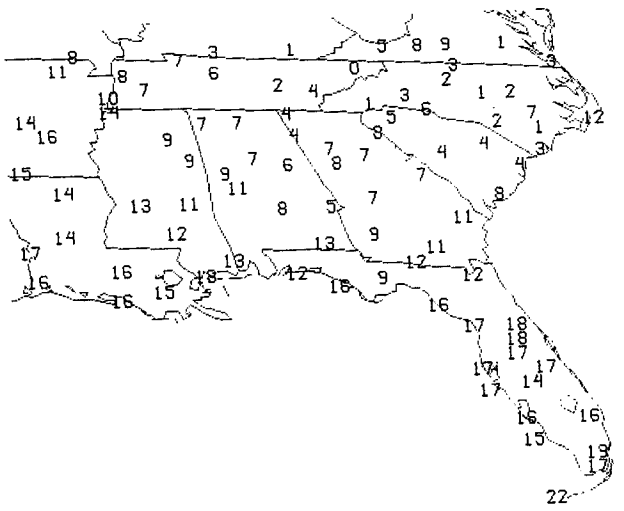

FIG. 6. Surface temperatures (°C) at 1100 UTC 26 October 1992.

tation System), provides digital satellite imagery to selected NWS offices via the Internet (Schrab et al. 1994). A "fog product" derived from *GOES-7* has been made available on RAMSDIS that is similar to the difference images described here. RAMSDIS will provide forecasters the opportunity to become familiar with the digital display of satellite imagery prior to the implementation of the Advanced Weather Interactive Processing Systems (AWIPS) in the late 1990s.

5. Estimation of fog thickness

After some experience with the bispectral imagery, it was observed that the interior portions of extensive fog and stratus clouds seemed to be associated with larger brightness difference (ΔB) values. Fog depth is generally thought to be thicker in the interior part of the cloud and thinner toward the edges. These observations of spatial brightness variations suggested that quantitative estimates of fog depth could be extracted from the IR difference imagery. This hypothesis is supported by calculations from Yamanouchi et al. (1987) that showed an increase in the brightness temperature difference between NOAA AVHRR CHs 3 and 4 as the thickness of water clouds increase.

a. Development of the regression equation

A sample of 80 observations was then collected in which the thickness of the fog layer was determined from aircraft pilot reports (PIREPs), along with a representative ΔB value at the same location. The data were collected on 39 days between July 1988 and November 1990 from 0900 to 1200 UTC. A plot of the results along with a linear regression line of best fit is shown in Fig. 2. A good relationship is observed, with a correlation coefficient of 0.78. The dashed line in Fig. 2 is an approximation of the data from Yamanouchi (1987) calculated for water clouds with a median drop diameter of 8 μm and a cloud temperature of 240 K. The drop diameter used in the study is typical for fog droplets (e.g., Byers 1965). There is excellent agreement between the two lines.

In the observed *GOES-7* data sample shown in Fig. 2, the fog thickness was estimated from the difference of the cloud-top heights [reported in feet above mean sea level (MSL)] obtained from PIREPs and the height of a nearby surface-observing station. The base of the cloud was assumed to be at the ground since visibilities were required to be 0.5 miles (0.8 km) or less to be included in the sample. Since most aircraft reports are received after sunrise, there is usually a time lag of at least 2–3 h between the satellite image and the PIREPs. As a result, the fog thickness values obtained from Fig. 2 are probably biased toward worst case values, since fog normally is thickest around sunrise (e.g., Findlater 1985).

Both color and black and white enhancement tables were then developed to display the fog depth in intervals of 200 m in a "step-wedge" pattern. The SIR-LIR imagery is normally smoothed over a 5 × 5 array so that patterns in the enhanced image can be more easily interpreted. This smoothing tends to distort the original fog boundaries somewhat, and smaller, thinner fog patches are sometimes reduced or eliminated.

An independent dataset of 28 cases was then collected between 1 August 1991 and 2 January 1992 to validate the enhancement technique. Fog thickness was determined in the same manner described above. The mean absolute error was 64 m (204 ft). The correlation between the satellite and aircraft estimates of cloud depth was good, with a correlation coefficient of 0.94.

b. Forecasting fog clearing time

A technique to determine the time required for fog dissipation (in hours after sunrise) from enhanced GOES visible imagery was developed by Gurka (1978b). Digital brightness values were determined over an area of fog and stratus and compared with the corresponding brightness of adjacent cloud-free land. The differences in these brightness values were found to be related to the time required for the fog to clear, as determined from surface and satellite observations. The technique requires visible images at about 1.5 h after sunrise.

The bispectral IR technique for estimating fog depth described in the previous section can also be used to estimate clearing time for radiation fogs. Dissipation time can be estimated from fog depth based upon methods developed by Wood (1938). Wood determined the thickness of stratus clouds from aircraft sounding data at three separate locations and compared them to the time required for the clouds to clear. His results are shown in Fig. 3. The data show that a thickness of 600 m, for example, usually requires 4–6 h to

clear. This approach will obviously not work for advection fog in which the clouds are steadily replenished by the low-level winds. The advantage of using the bispectral IR imagery to estimate fog-clearing time is that it provides information needed for short-range forecasts much earlier than the enhanced visible method.

6. Examples

a. 26 October 1992

On the night of 25–26 October 1992, radiation fog developed in the interior of northern Florida and along the northern coast of the Gulf of Mexico. By 1100 UTC, visibilities were 1 mile (1.6 km) or less over much of northern Florida and south-central Georgia and 3–5 miles (5–8 km) elsewhere along the Gulf Coast (Fig. 4). The *GOES-7* CH8 IR image at 1130 UTC is shown in Fig. 5. Regions of dense fog in northern Florida to southern Georgia (A) appear dark, whereas clear regions (B) are lighter gray or white. The dark appearance of the fog is attributed to radiation originating from the warm top of the fog layer, which is located within a temperature inversion (Gurka 1980). The land surface has a lighter gray appearance in fog-free areas due to radiational cooling. The fog in southern Louisiana (C) is not as distinct, but its northern border is still visible. Both regions of fog have identifiable boundaries over land because of the temperature contrast, but their extent in coastal areas is not evident.

Note that in clear regions in Fig. 5 (B), surface features such as lakes and rivers are easily seen, but they are obscured where fog is present. The dark region in extreme southern Florida (D) is believed to be a result of the warm water of the Everglades swamp, since it does not change its appearance from image to image. Figure 6 shows the surface temperatures (°C) as reported by observing stations at 1100 UTC. Much cooler conditions can be found in the northern clear areas (0°–10°C) than where fog is present (10°–18°C).

A *GOES-7* CH12 IR image at 1130 UTC is shown in Fig. 7. Due to the lower resolution of this channel, these images have a much grainier appearance than the CH8 image in Fig. 5. The area of fog described above is also somewhat colder in CH12, as evidenced by the lighter gray shades in Fig. 7. The cooler CH12 temperatures result in a loss of contrast between the fog and surrounding clear regions. In some warm season fog situations, CH12 can provide much better delineation of the boundary of the fog, but in this case, temperatures in the clear regions over land were too cool. However, the CH12 images do provide good depiction of the eastern edge of the fog off the east coast of Florida (E) and suggest that the fog in west-central Florida (F) does not extend offshore.

A comparison of observed brightness temperatures at 1130 UTC for CHs 8 and 12 across the fog deck along G-G′ (in Fig. 5) is shown in Fig. 8. CH12 (dotted line) is significantly cooler (2–4 K) than CH8, where dense fog was present (pixel numbers 20–40) and slightly cooler (1–2 K) in the Florida panhandle, where only minor visibility restrictions were observed. Note that the CH8 temperatures in the fog-free area of the Florida panhandle (282–283 K) are in good agreement with surface observations of 9°C (282 K) from Fig. 4. In the Atlantic Ocean east of Florida, the temperature differences are negligible, although CH8 was slightly cooler than CH12. It is apparent that by obtaining the difference between the two channels, discrimination of the fog will be less ambiguous and less dependent on ambient surface temperature conditions.

The unsmoothed SIR-LIR image derived at 1130 UTC is shown in Fig. 9. The images re enhanced so that fog and stratus clouds are depicted as white to light gray. The areas of dense fog supported by surface observations over Florida and southeast Georgia (A) are clearly depicted. The fog in Louisiana (C) is more subtle but still evident. The medium gray area in eastern Georgia and South Carolina (H) shows the presence of shallow, nonopaque fog with surface visibilities from 2 to 6 miles (3 to 10 km). Darker shades of gray represent fog-free areas. Note that the dark region seen in Fig. 5 over the Everglades swamp in south Florida (D) appears dark in Fig. 9, indicating clear conditions. The black patches in Louisiana, Arkansas, and east Texas show a reversal in the CH8–CH12 temperature relationship, suggesting the presence of cirrus clouds.

A smoothed image enhanced with a step-wedge pattern to show approximate fog depth at 1130 UTC is shown in Fig. 10. The outer dark gray shade represents depths of less than 200 m, the light gray 200–400 m, and the black 400–600 m. Aircraft PIREPs from 1324 to 1544 UTC indicated cloud tops at 300–360 m (1000–1200 ft) at Orlando (A) and Gainesville (B), Florida, decreasing to 150 m (500 ft) at Tampa (C), Florida, near the Gulf of Mexico. In southern Louisiana, the fog-layer top was estimated by aircraft at 150 m (500 ft) at both Baton Rouge (D) and Lafayette (E). The PIREPs show that the satellite product may have overestimated the fog depth slightly but provided a reasonably good description of the conditions.

Inspection of visible imagery throughout the morning (not shown) indicated that the thickest portion of the fog depth drifted toward the southwest and finally cleared by around 1600 UTC (1200 EDT). The use of Fig. 3 for forecasting clearing time would have required about 4.5 h to clear, assuming a maximum thickness of 500 m. The actual clearing time after sunrise was about 5.5 h. The low sun angle present in late October probably accounts for this discrepancy.

b. 30 August 1994

Based on improvements in IR resolution and image frequency, the *GOES-8* satellite was expected to provide considerably better nighttime fog-detection capabilities. An example of this improvement was dra-

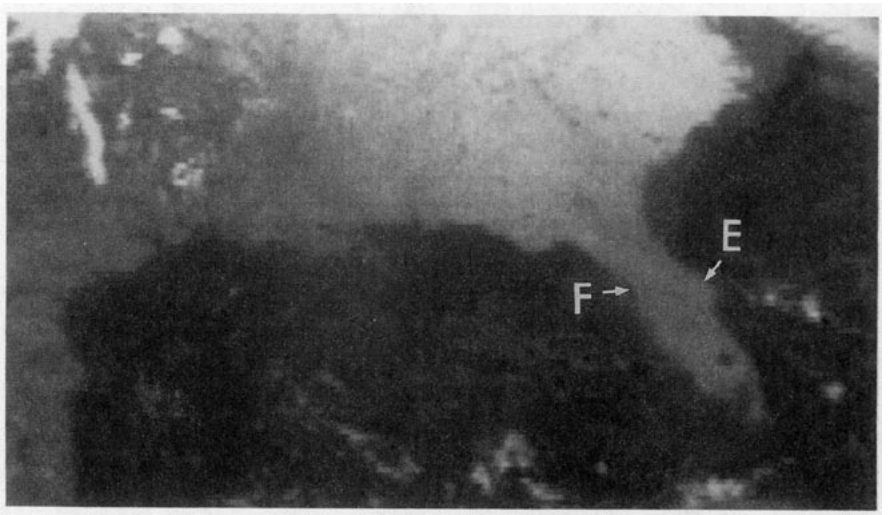

FIG. 7. *GOES-7* CH12 (3.9 μm) IR image at 1130 UTC 26 October 1992.

matically seen on the morning of 30 August 1994 over the central and southern Appalachian Mountains. Light winds and a cool, moist air mass allowed considerable radiation fog to develop in many interior valleys. Observations at 1000 UTC (0600 EDT) indicated visibilities of less than 0.25 miles (400 m) at many locations in West Virginia (Fig. 11) and 3–5 miles (5–8 km) to the south.

Bispectral difference (SIR-LIR) images created from both *GOES-8* and *GOES-7* and remapped to a common Mercator projection are shown in Fig. 12. While the *GOES-7* image suggests that fog or low clouds are present in much of the region, its boundaries and areal extent are indefinite. The *GOES-8* image provides a dramatically better depiction of the specific valleys obscured by fog. The large black patches are cirrus clouds

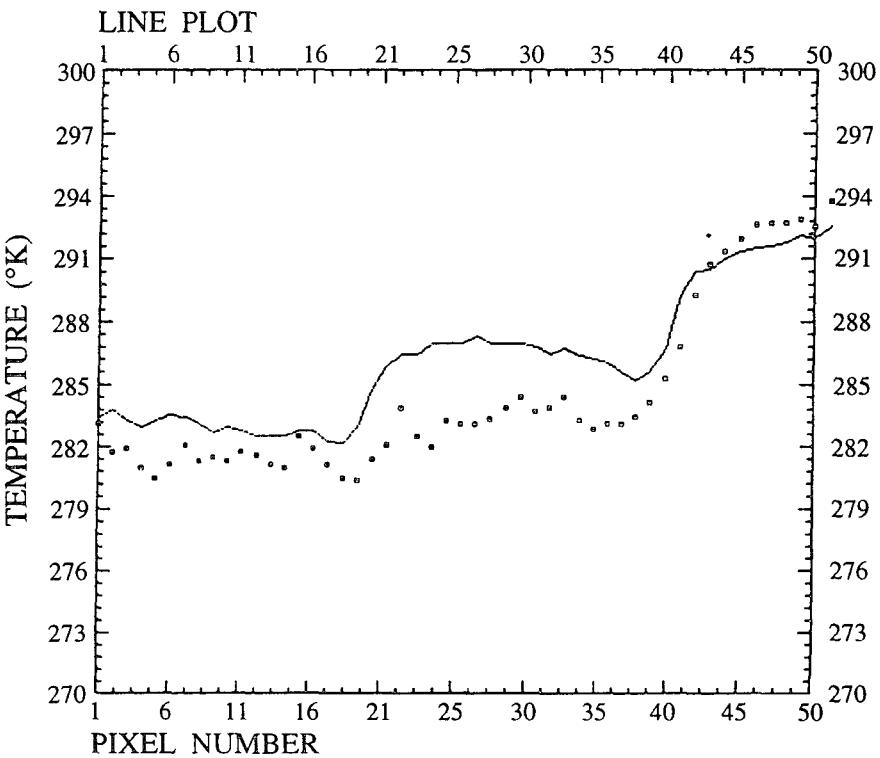

FIG. 8. A plot of brightness temperatures (K) along the line G-G′ in Fig. 5. Solid line is from *GOES-7* CH8 (11.2 μm), and the dotted line is from CH12 (3.9 μm) IR.

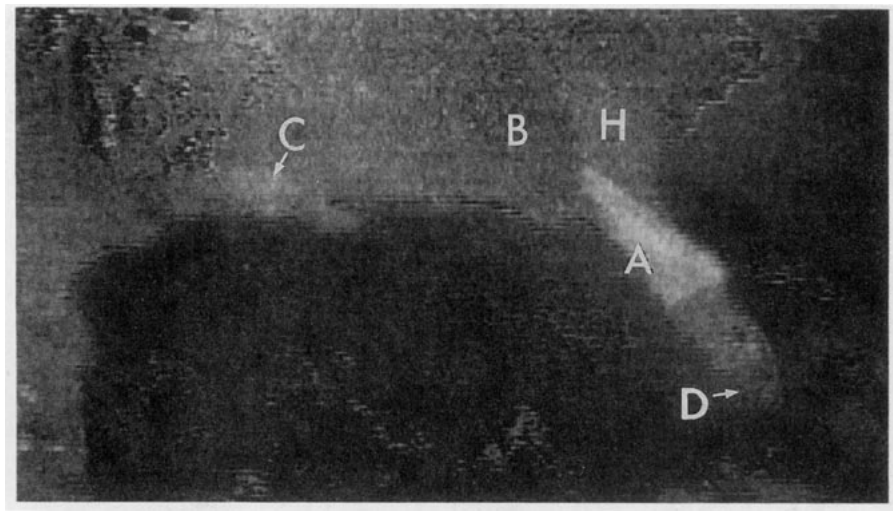

FIG. 9. Unsmoothed *GOES-7* IR difference image based on subtraction of *GOES-7* CH12 from CH8 brightness temperatures at 1130 UTC 26 October 1992.

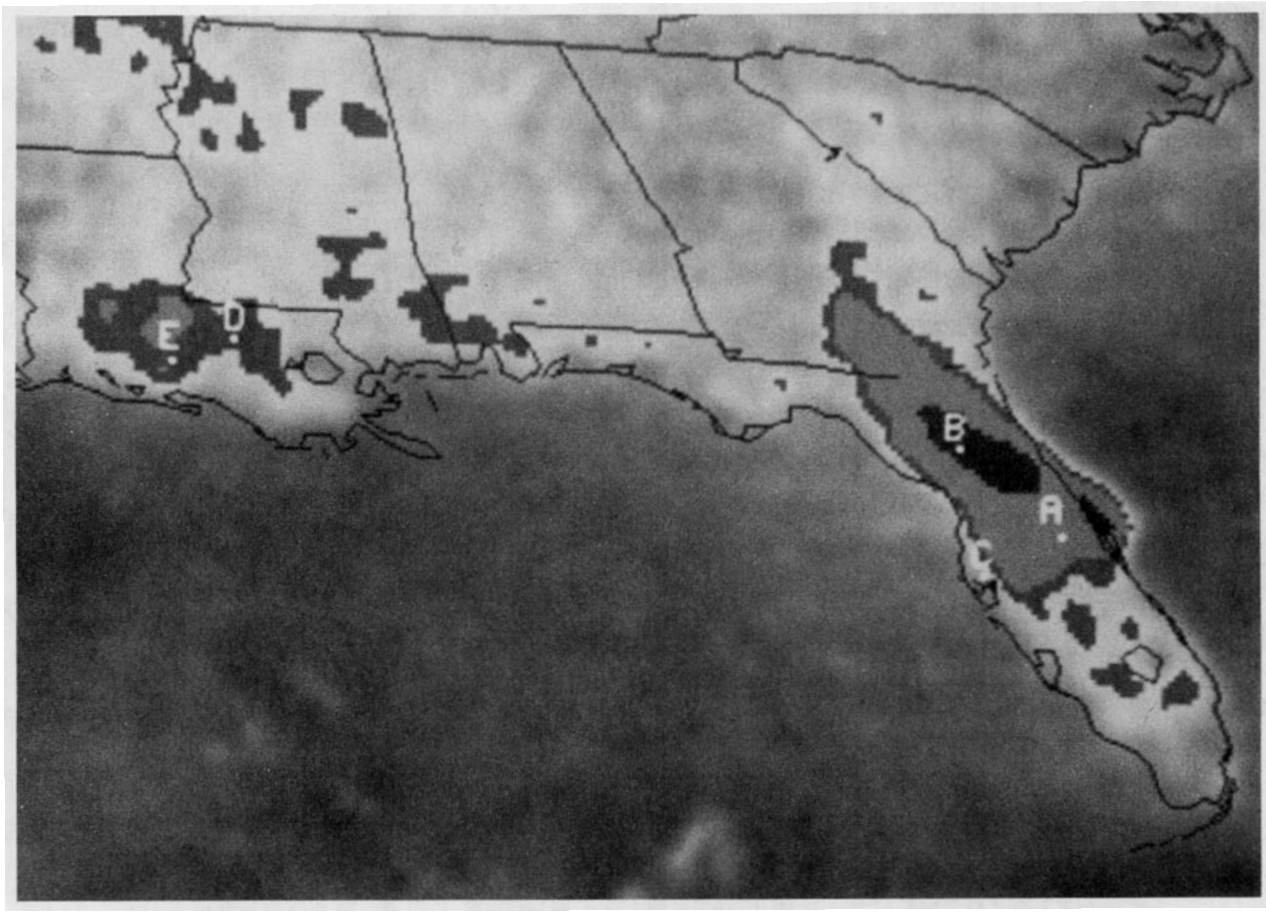

FIG. 10. Smoothed *GOES-7* bispectral difference image at 1130 UTC 26 October 1992, enhanced to show approximate fog thickness in 200-m intervals. Medium gray represents less than 200 m, light gray represents 200–400 m, and black represents 400–600-m depth.

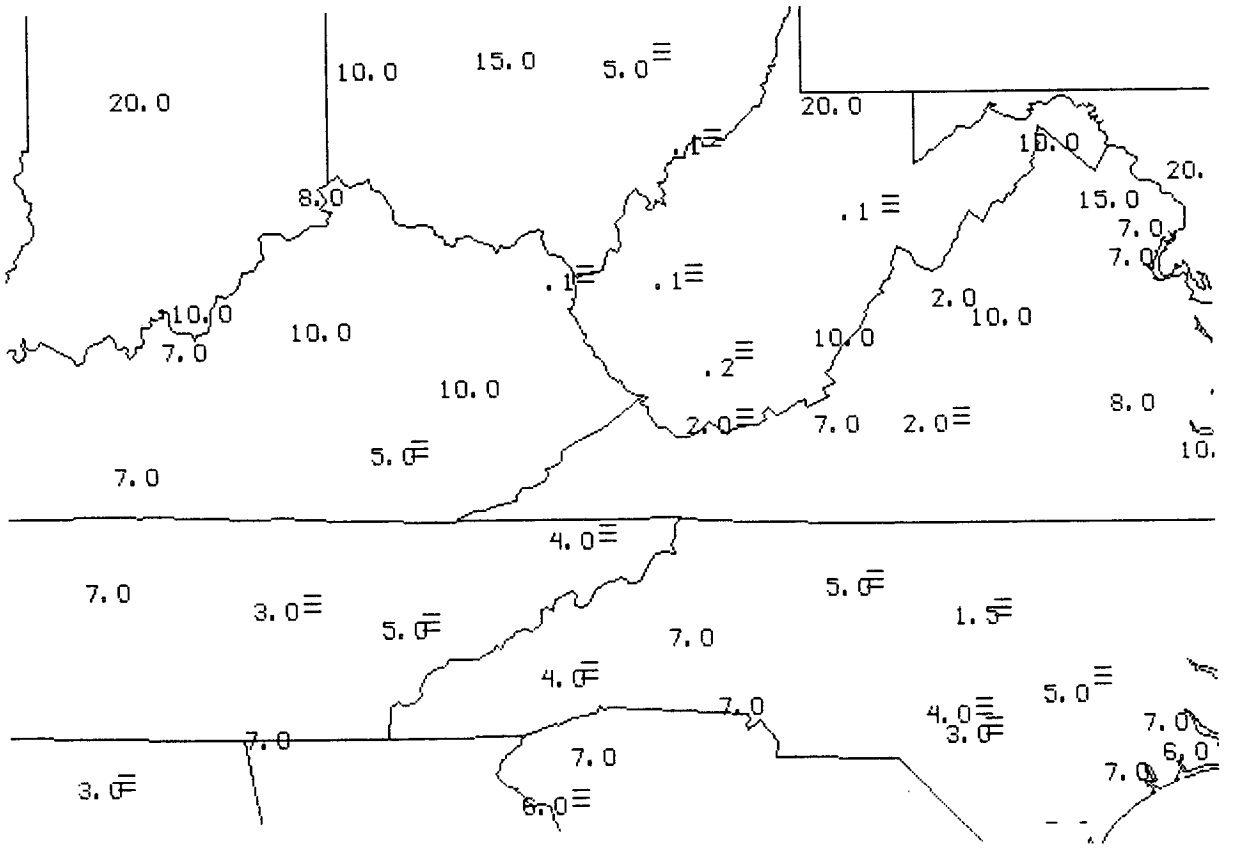

FIG. 11. Surface observations of current weather and visibility (miles) at 1000 UTC 30 August 1994.

that likely mask other fog-covered valleys. The cirrus is clearly seen in the *GOES-8* CHs 2 and 4 images at 1000 UTC in Fig. 13. Figure 13 suggests the presence of some low clouds, but not nearly to the extent shown in Fig. 12.

A *GOES-8* visible image valid 2.5 h later (1230 UTC) is shown in Fig. 14. Some narrow fingers of valley fog can be seen that were not observed in the SIR-LIR image. A few of these could have developed in the time interval between images. In general, however, the *GOES-8* IR difference image provided a strikingly accurate view of low cloud coverage prior to sunrise. The availability of this type of imagery would significantly improve early morning aviation forecasts.

A fog depth enhancement for *GOES-8* has been developed by modifying the existing enhancement described above. Comparisons of spatial average temperatures by the author indicate that *GOES-8* CH2 is about 2 K colder than the equivalent *GOES-7* CH12. Much of this can be attributed to a difference in the spectral responses the two channels (CH12 is a sounder channel and thus has a more narrow spectral response with less absorption by water vapor) (M. Weinreb 1995, personal communication). Based on the average observed temperature difference, adjustments have been made to the *GOES-8* enhancement to display more accurate fog thickness.

7. Versatility and limitations of bispectral imagery

Experience with the SIR-LIR-derived imagery has shown that it is very versatile with respect to the types of terrain and underlying surface temperatures over which it can effectively identify the presence of stratus and fog. In addition to the above examples, the bispectral technique is useful over open-ocean areas such as the North Atlantic, mountainous coastal regions such as along the Pacific coast, and deep, snow-covered valleys such as in the Rocky Mountains. Examples of these were shown in Ellrod (1994).

One difficulty observed with cold, snow-covered surfaces is the increase in instrument noise that accompanies surface temperatures much less than 0°C. Nevertheless, the signal present from stratus clouds is usually strong enough to be observed until T is less than −20°C based on a *GOES-7* case over the Rockies on 4 February 1993 (Ellrod 1994).

Occasionally, certain types of soils will produce the same signature as fog or stratus in SIR-LIR images in cloud-free conditions. A pronounced example of this

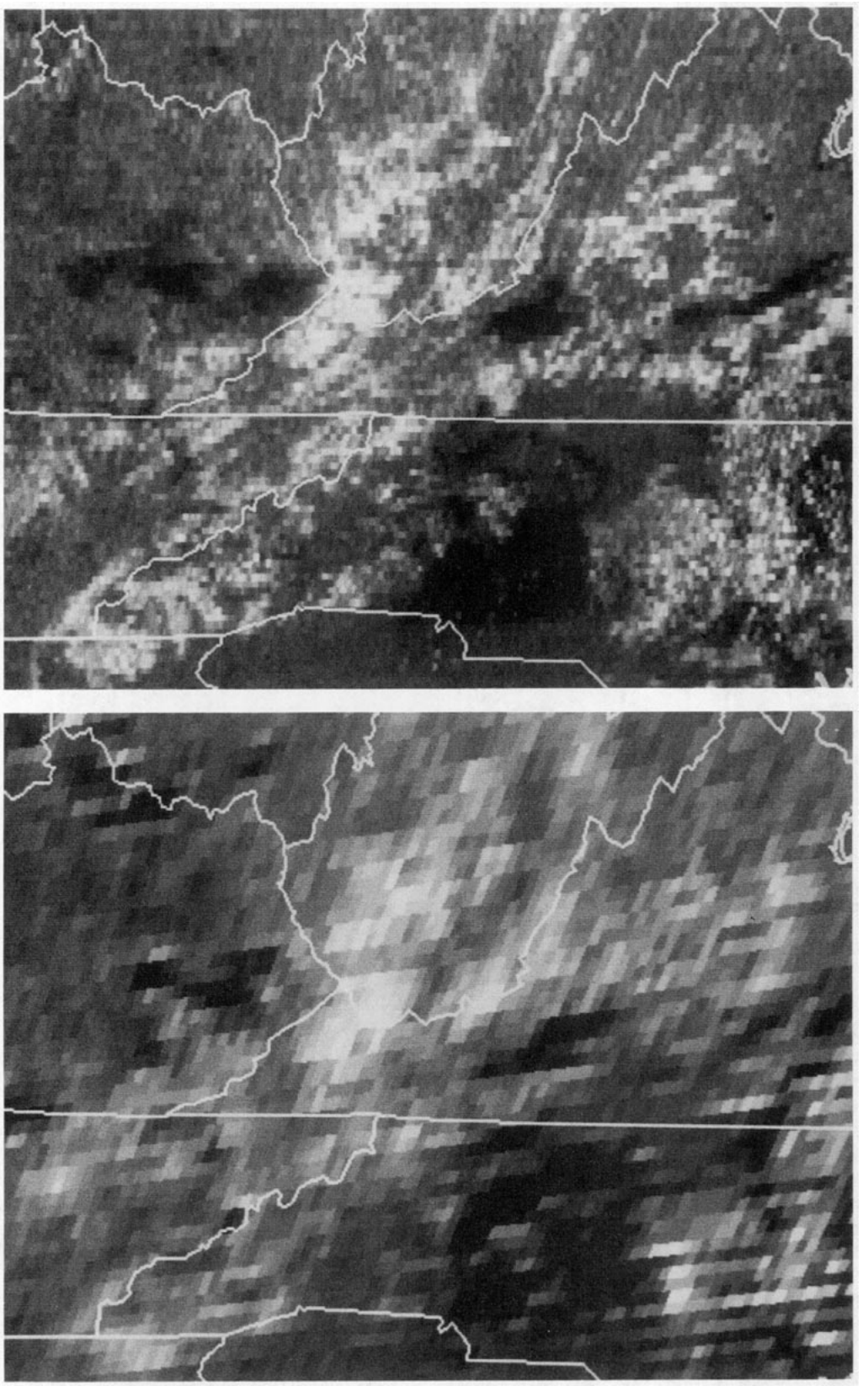

FIG. 12. Bispectral IR difference images from (a) *GOES-8* at 1000 UTC and (b) *GOES-7* at 1030 UTC 30 August 1994. The images are remapped to a Mercator projection.

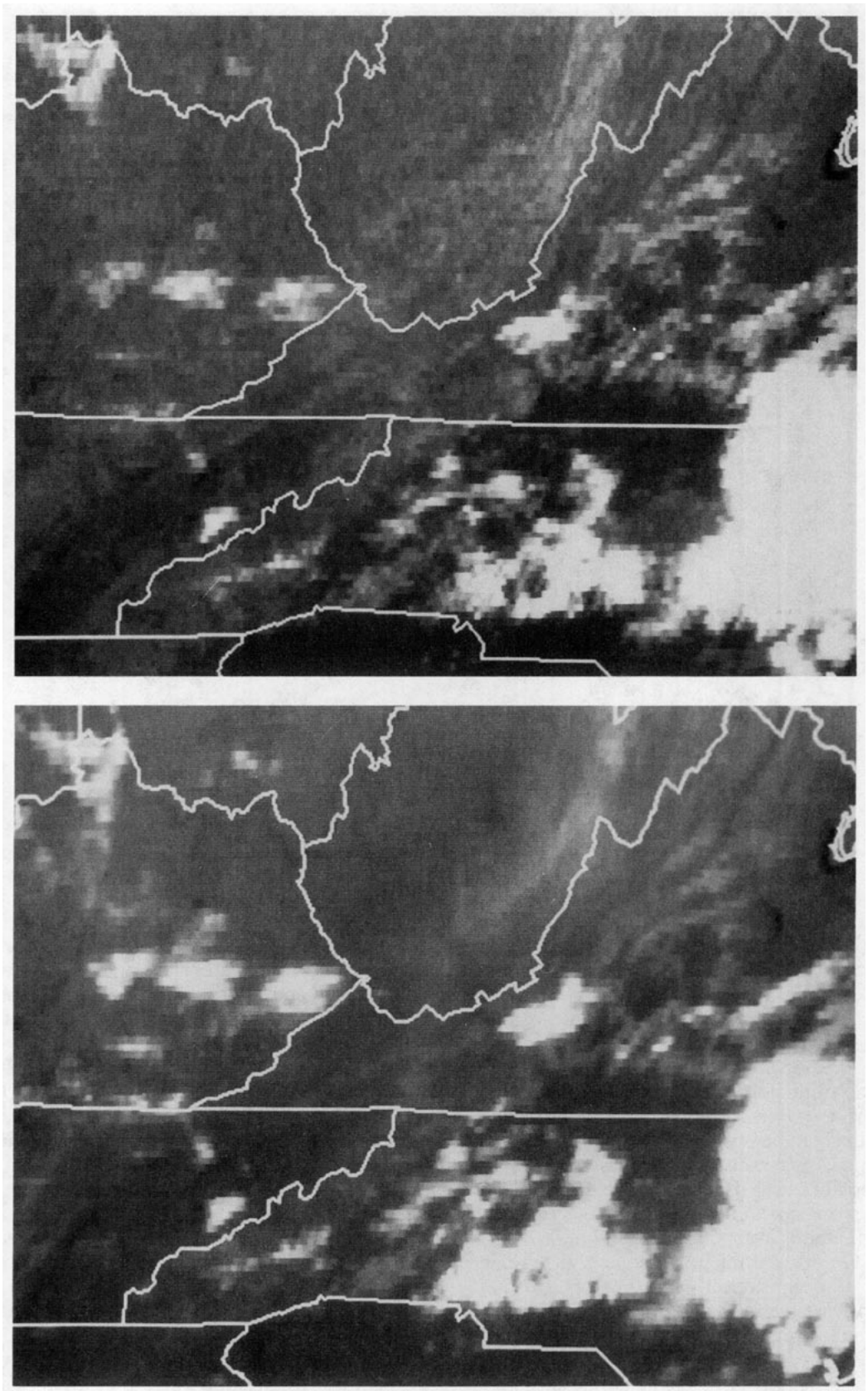

FIG. 13. *GOES-8* images (remapped to Mercator) from (a) CH2 (3.9 μm) (top) and (b) CH4 (10.7 μm) at 1000 UTC 30 August 1994.

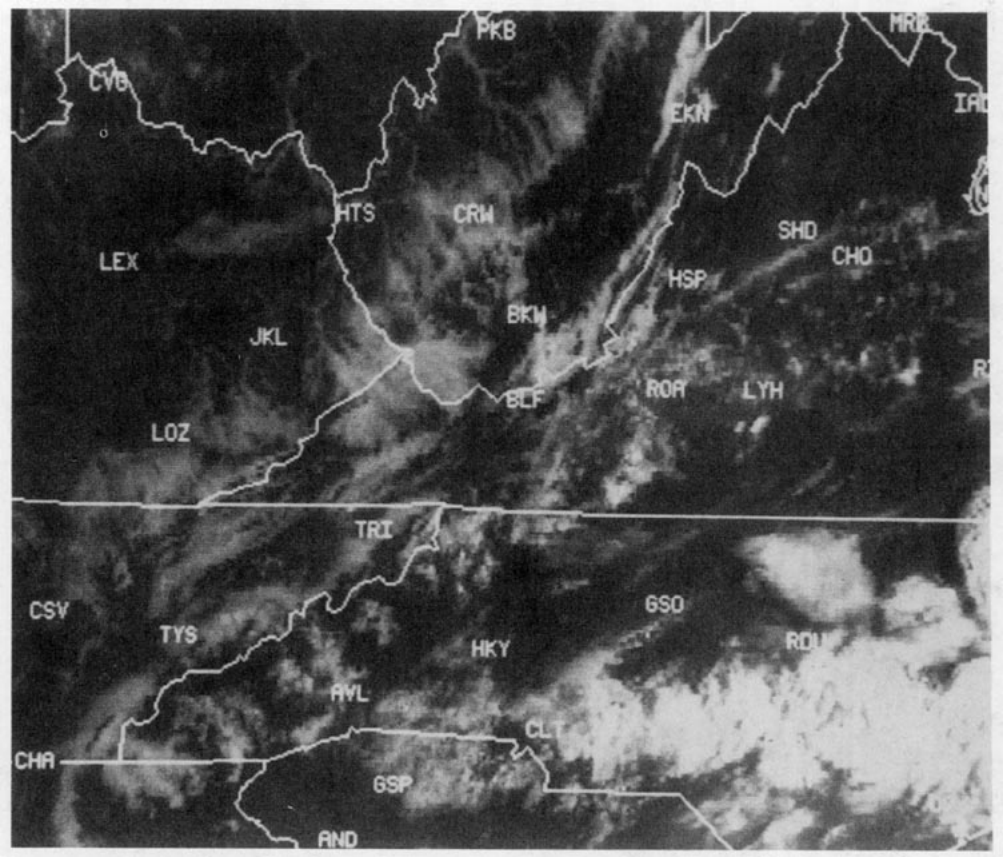

FIG. 14. Visible image from *GOES-8* (remapped to Mercator) at 1230 UTC 30 August 1994. Three-letter identifiers correspond to locations of surface observations shown in Fig. 11.

frequently occurs just north of the Gulf of California, to the east of the Colorado River. This "false alarm" is nearly always seen at this location even though fog is seldom observed. More subtle examples can occasionally be seen in the High Plains and some valleys in the southwestern United States. Sutherland (1986) found that there are considerable differences in the calculated IR emissivity of soil types versus wavelength. At 3.75 μm, for example, coarse sand has an emissivity of 0.793, while vegetated regions have an emissivity of 0.963. This difference in the radiative properties of the soil likely accounts for the bogus fog signatures.

Layers of very thin stratus or fog ($\ll$100 m thick) are not as likely to be observed by means of bispectral difference imagery because the temperature differences between the SIR and LIR channels are too small. This is a result of the small differences in emissivity shown in Fig. 1 for clouds much less than 100 m.

As noted in the example in section 6b, the presence of higher cloud layers usually obscures any low clouds normally observable in the IR difference images. The use of animation reduces this problem considerably, allowing a view of low clouds between breaks in high cloud cover, except in cases of extensive, multilayered cloud systems.

Higher-based stratiform clouds such as stratocumulus or altostratus often resemble fog or low stratus in SIR-LIR imagery. An example of this can be seen in central Virginia, in Figs. 11–14. A few differences between the cloud types have been noted to aid in detection of the lowest clouds. The brightness of fog and stratus tends to be more pronounced than higher clouds. Low stratus also has a smooth appearance, while higher clouds are more mottled. These effects are likely caused by more uniform drop-size distributions in fog and stratus, lack of convection, and an absence of breaks or thin spots in the overcast at subpixel resolution. Work is under way to upgrade the IR difference product by automatically eliminating higher-based clouds from the images.

8. Summary and conclusions

A technique that detects the presence of fog or low stratiform clouds at night from the digital subtraction of brightness or brightness temperatures for two GOES IR window channels (at 10.7–11.2- and 3.9-μm wavelengths) has been described. The resulting difference imagery is effective over a wide range of terrain and temperature regimes, provided that the fog or stratus are not obscured by higher cloud layers.

A step-wedge enhancement technique for quantitative estimates of fog thickness based on the smoothed bispectral image is believed to be accurate to less than 100 m. The depth estimates can then be used by aviation forecasters to help determine the approximate dissipation time of the fog prior to the availability of other data sources such as pilot reports or rawinsondes. The instrument noise inherent in the GOES SIR (3.9 μm) channels requires considerable smoothing to make the fog-depth product useful.

There are some limitations to the effectiveness of the derived imagery. The poor subpoint resolution (13.8 km) of *GOES-7* SIR imagery does not allow detection of narrow fingers of valley fog. These types of fog situations are more easily seen with *GOES-8* data. There is difficulty in resolving very shallow fog layers with GOES because the small temperature differences observed between the two IR channels (1°–2°C) are often within the instrument noise of the SIR channel, especially in winter. Regardless of which satellite is used, bispectral imagery sometimes cannot differentiate between fog, stratocumulus, or altocumulus layers. Some subtle differences are apparent in the imagery to aid detection. Fog typically has a more distinct brightness and is smoother in appearance. By combining temperature information from the LIR channel, identification of fog should be less ambiguous.

Bispectral IR image differencing techniques using the 3.9- and 10.7–11.2-μm channels from GOES show considerable promise in the detection of hazardous fog and low clouds for aviation and marine weather forecasting. The improvements in the GOES satellite instruments that have come to pass will encourage more widespread use of these derived products in the coming years.

Acknowledgments. The author would like to thank Frances Holt and Thomas Kleespies of the National Environmental Satellite Data, Information Service (NESDIS), Doug Mathews of NWS/NAWAU in Kansas City, Jim Gurka of the NWS Boston, and George Bancroft and Dave Feit of the NMC Marine Forecast Branch in Washington for their comments on previous versions of this paper. Lori Paschal assisted with the text and layout. Phil Golden of PRC processed the photographs.

REFERENCES

Allen, R. C., P. A. Durkee, and C. H. Wash, 1990: Snow-cloud discrimination with multispectral satellite measurements. *J. Appl. Meteor.*, **29,** 994–1004.

Anderson, R. K., and Coauthors, 1974: Application of meteorological satellite data in analysis and forecasting. ESSA Tech. Report NESC 51, U.S. Dept. of Commerce, Washington, DC, p. 6-B-1.

Byers, H. R., 1965: *Elements of Cloud Physics.* University of Chicago Press, 142–143.

Clark, J. D. (Ed.), 1983: *The GOES User's Guide.* U.S. Dept. of Commerce, National Oceanic and Atmospheric Administration (NOAA), Washington, DC, 7–3.

d'Entremont, R. P., 1986: Low- and midlevel cloud analysis using nighttime multispectral imagery. *J. Clim. Appl. Meteor.*, **25,** 1853–1869.

——, and L. W. Thomason, 1987: Interpreting meteorological satellite images using a color-composite technique. *Bull. Amer. Meteor. Soc.*, **68,** 762–768.

Ellrod, G. P., 1991: Nighttime fog detection with bi-spectral GOES-VAS imagery. *Proc., Fourth Int. Conf. on Aviation Weather Systems,* Paris, France. Amer. Meteor. Soc., 71–75.

——, 1994: Detection and analysis of fog at night using GOES multispectral infrared imagery. NOAA Tech. Rep. NESDIS 75, U.S. Dept. of Commerce, Washington, DC, 22 pp.

——, E. Maturi, and J. Steger, 1989: Detection of fog at night using dual channel GOES-VAS imagery. *Proc. 12th Conf. on Weather Analysis and Forecasting,* Monterey, CA, Amer. Meteor. Soc., 515–520.

Eyre, J. R., J. L. Brownscombe, and R. J. Allam, 1984: Detection of fog at night using Advanced Resolution Radiometer (AVHRR) imagery. *Meteor. Mag.*, **113,** 266–271.

Findlater, J., 1985: Field investigations of radiation fog formation at outstations. *Meteor. Mag.*, **114,** 187–201.

Gurka, J. J., 1980: Observations of advection–radiation fog formation from enhanced IR satellite imagery. *Proc., Eighth Conf. on Weather Forecasting and Analysis,* Denver, CO, Amer. Meteor. Soc., 108–114.

——, 1978a: The role of inward mixing in the dissipation of fog and stratus. *Mon. Wea. Rev.*, **106,** 1633–1635.

——, 1978b: The use of enhanced visible imagery for predicting the time of fog dissipation. *Proc., Conf. on Weather Forecasting and Analysis and Aviation Meteorology,* Silver Spring, MD, Amer. Meteor. Soc., 343–346.

Hunt, G. E., 1973: Radiative properties of terrestrial clouds at visible and infrared thermal window wavelengths. *Quart. J. Roy. Meteor. Soc.*, **99,** 346–369.

Kidder, S. Q., and H.-T. Wu, 1984: Dramatic contrast between low clouds and snow cover in daytime 3.7-μm imagery. *Mon. Wea. Rev.*, **112,** 2345–2346.

McClain, E. P., W. G. Pichel, C. C. Walton, Z. Ahmad, and J. Sutton, 1983: Multi-channel improvements to satellite-derived global sea surface temperatures. *Adv. Space Res.*, **2,** 43–47.

Menzel, W. P., and J. F. W. Purdom, 1994: Introducing GOES-I: The first of a new generation of Geostationary Operational Environmental Satellites. *Bull. Amer. Meteor. Soc.*, **75,** 757–781.

Montgomery, H. E., and L. W. Uccellini, 1985: VAS demonstration: (VISSR atmospheric sounder) description and final report. *NASA Reference Publication 1151,* National Aeronautics and Space Administration, 198 pp.

Schrab, K. J., D. Molenar, J. F. W. Purdom, L. Dunn, and B. Colman, 1994: The use of digital satellite data via a menu system in NWS offices. Preprint Volume, *Seventh Conf. on Satellite Meteorology and Oceanography,* Monterey, CA, Amer. Meteor. Soc., 448–451.

Suomi, V. E., R. Fox, S. S. Limaye, and W. L. Smith, 1983: McIDAS III: A modern interactive data access and analysis system. *J. Climate. Appl. Meteor.*, **22,** 766–778.

Sutherland, R. S., 1986: Broadband and spectral emissivities (2–18 μm) of some natural soils and vegetation. *J. Atmos. Oceanic Technol.*, **3,** 199–202.

Wood, F. B., 1938: The formation and dissipation of stratus clouds beneath turbulent inversions. *Bull. Amer. Meteor. Soc.*, **19,** 97–103.

Yamanouchi, T., K. Suzuki, and S. Kawaguchi, 1987: Detection of clouds in Antarctica from infrared multispectral data of AVHRR. *J. Meteor. Soc. Japan,* **65,** 949–961.